ACS APPLIED MATERIALS & INTERFACES

Research Article

www.acsami.org

A Near-Infrared Dithieno[2,3-*a*:3′,2′-*c*]phenazine-Based Organic Co-Sensitizer for Highly Efficient and Stable Quasi-Solid-State Dye-Sensitized Solar Cells

Xuefeng Lu, Tian Lan, Zhenwen Qin, Zhong-Sheng Wang, and Gang Zhou*

Laboratory of Advanced Materials and Department of Chemistry, Fudan University, Shanghai 200438, People's Republic of China

Supporting Information

ABSTRACT: A novel near-infrared (NIR) organic sensitizer FNE53 with a strong electron-withdrawing unit, dithieno[2,3-*a*:3′,2′-*c*]phenazine, has been designed and synthesized for quasi-solid-state dye-sensitized solar cells (DSSCs). By simply fusing the two thiophene rings on quinoxaline unit in sensitizer FNE48, the intramolecular charge transfer (ICT) band bathochromically shifts from 542 nm for FNE48 to 629 nm for FNE53 in toluene solution. The absorption spectrum of sensitizer FNE53 covers the whole visible region and extends to the NIR region, which exhibits complementary absorption profile to another organic dye FNE46 based on quinoxaline. When FNE46 and FNE53 are used as cosensitizers for metal-free cocktail-type quasi-solid-state DSSCs, sensitizer FNE53 not only extends the photoresponse range but also suppresses the intermolecular interactions among the dye molecules. Therefore, the cocktail-type quasi-solid-state DSSC displays much higher IPCE value compared with that for the DSSC sensitizer based on FNE53 and a broader IPCE response in comparison to that for the DSSC sensitizers based on FNE46, respectively. After the molar ratio between the two cocktail dyes is optimized, the highest energy conversion efficiency of 8.04% is achieved in a metal-free quasi-solid-state DSSC cosensitized with FNE46 and FNE53, which exhibits good long-term stability after continuous light soaking for 1000 h.

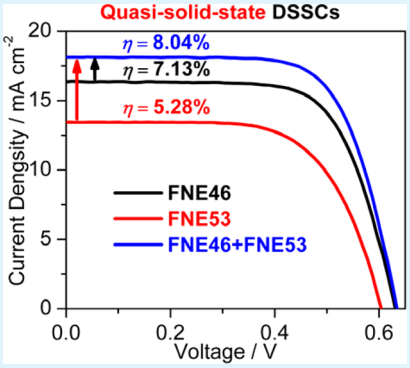

KEYWORDS: *phenazine, near-infrared, cosensitizer, quasi-solid-state, dye-sensitized solar cells*

INTRODUCTION

Dye-sensitized solar cells (DSSCs) have attracted ever-increasing attention as a renewable energy source due to their efficient energy conversion and relatively low cost of production.[1−4] To improve the DSSC performance by harvesting more solar light, researchers have concentrated great effort on developing panchromatic dyes with absorption spectra extending into the near-infrared (NIR) region.[5] Several organic NIR dyes have been designed and reported, such as organic sensitizers containing porphyrin,[6] squaraines,[7] phenoxazine,[8] perylene,[9] boradiazaindacene,[10] phthalocyanine,[11] tetrahydroquinoline,[12] and diketopyrrolopyrrole[13] units. However, in contrast to their wide photocurrent response, most of the reported NIR dyes have unsuitable highest occupied molecular orbitals (HOMOs), lowest unoccupied molecular orbitals (LUMOs), or both, which results in insufficient driving forces for the dye regeneration or the electron injection from the excited dye molecules to the titania conduction band.[12−14] Consequently, NIR-dye-sensitized DSSCs tend to have a low incident photon-to-current conversion efficiency (IPCE) and a low open-circuit voltage (V_{oc}).[8−15] Moreover, some NIR-dye-based DSSCs display unsatisfactory stability, which is probably caused by the decomposition of the NIR dyes themselves.

To overcome the disadvantages, cosensitization, an alternative approach for panchromatically harvesting sunlight, has been proven to be an effective method for enhancing the DSSC performance.[16] Such cocktail dyes involve two or more sensitizers that have complementary absorption spectral coverage.[17] A classic example is zinc-porphyrin dye YD2-*o*-C8 and organic dye Y123 cosensitized DSSC which produced an efficiency record of 12.3%.[18] However, until now, most of the highly efficient cosensitized DSSCs have combined at least a ruthenium-complex dye or a zinc-porphyrin dye.[16−20] Such metal-based sensitizers[16−21] have always suffered from some problems such as expensive raw materials and complicated syntheses. In comparison to metal-based sensitizers, metal-free organic sensitizers[22] have attracted much attention for practical applications due to their unique advantages such as having a low cost of production, being environmentally friendly, and having tunable optoelectronic properties via molecular engineering. However, relatively few efficient cosensitized DSSCs based on organic dyes have been reported.[23] Moreover, most highly efficient cosensitized DSSCs have been realized with volatile organic liquid electrolytes,[16,18,23] which may limit their outdoor applications. Alternatively, quasi-solid-state DSSCs with nonflowing and nonvolatile electrolyte have

Received: August 10, 2014
Accepted: October 7, 2014
Published: October 7, 2014

shown greatly improved long-term stability because there is less or no possibility of electrolyte leakage.[24] Therefore, in view of promising commercial application, highly efficient and stable cosensitized DSSCs with quasi-solid-state electrolyte are still pursued.

Most recently, a quinoxaline unit has been embedded into the organic sensitizers as an auxiliary electron acceptor for efficient DSSCs by several groups.[25−30] We have also applied quinoxaline to construct organic dyes with single[31] and double[32] D−π−A'−π−A branches for expanding the sensitizer absorption band and improving the DSSC performance. In our previous studies, sensitizer FNE48 displays a maximum absorption wavelength at 542 nm in toluene solution.[32] However, due to the repulsion between the two thiophene rings linked at the 2,3-positions of the pyrazine unit (Chart 1),

Chart 1. Molecular Models of the Cores for Sensitizers FNE48 and FNE53

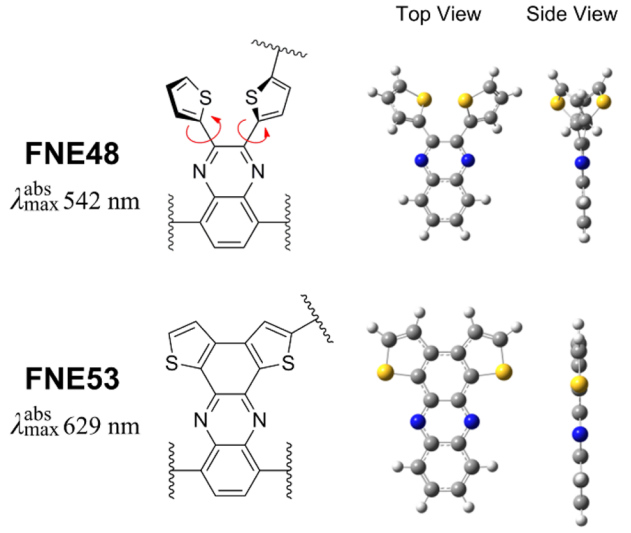

a molecular twist of around 44° exists between the thiophene and pyrazine rings, which has weakened the effective conjugation length and the intramolecular charge transfer (ICT) from the electron donating unit to the electron acceptor unit. Therefore, to further bathochromically shift the absorption band of the organic sensitizer, such a molecular twist should be minimized. Herein, we have designed and synthesized a neutral NIR sensitizer based on dithieno[2,3-*a*:3′,2′-*c*]phenazine, coded as FNE53 (Chart 2), for the construction of efficient quasi-solid-state DSSCs. In the new dye molecule, the two thiophene rings are chemically connected with a single bond, which leads to a fully coplanar structure for the central dithieno[2,3-*a*:3′,2′-*c*]phenazine core. As a result of better conjugation and facile ICT, the maximum absorption wavelength of sensitizer FNE53 bathochomically shifts to 629 nm by 87 nm, compared with that of sensitizer FNE48.[32] The quasi-solid-state DSSC based on the NIR sensitizer FNE53 exhibits a power conversion efficiency of 5.28% with a V_{oc} of 604 mV, which is a very promising V_{oc} value for quasi-solid-state DSSC based on organic NIR dye. Furthermore, another of our previously reported sensitizers, FNE46,[31] based on quinoxaline, exhibits an absorption maximum at 520 nm in toluene solution, which well compensates for the valley in the absorption spectrum for sensitizer FNE53. Therefore, when FNE53 and FNE46 were utilized as cocktail cosensitizers, the quasi-solid-state DSSC exhibited much higher IPCE value compared to that of FNE53 and broader IPCE response compared to that of FNE46, respectively. Consequently, a high conversion efficiency of 8.04% was achieved for the corresponding cocktail-type quasi-solid-state DSSC under AM 1.5 radiation (100 mW cm^{-2}), which was enhanced by 13 and 52% compared to those of the quasi-solid-state DSSCs based on sensitizers FNE46 and FNE53, respectively. Moreover, this metal-free cocktail-type quasi-solid-state DSSC exhibited good long-term stability after continuous light soaking for 1000 h.

RESULTS AND DISCUSSION

Molecular Design and Synthesis. Most metal-free organic dyes consist of a rod-like configuration, which always induces undesirable π−π stacking and intermolecular aggregation. Therefore, the excited electrons may be self-quenched, resulting in insufficient electron injection.[33] The construction of multidonors[34−36] or multiacceptors,[37−39] as well as double D−π−A branched dyes with "H"[40,41] or "X"[42] shape, has proved to be an effective method to reduce intermolecular interactions and thus retard charge recombination rate. To improve the light harvesting ability of X-shaped sensitizer FNE48, a fully coplanar core dithieno[2,3-*a*:3′,2′-*c*]phenazine is utilized in sensitizer FNE53 instead of the twisted 2,3-di(thien-2-yl)quinoxaline in sensitizer FNE48. Moreover, four octoxyl groups are incorporated into dye molecules to avoid the solubility problem during the synthesis procedure. The introduction of four linear alkyl chains is also beneficial to the inhibition of intermolecular aggregation and the decreasing of the charge recombination rate. Furthermore, according to our previous results, a broader and more intense charge transfer band is observed for sensitizer FNE48 with a single anchoring group in comparison to the other sensitizer containing double anchoring groups, which results in a higher light harvesting ability and a higher energy conversion efficiency.[32] Therefore, in this study, only the sensitizer with the single anchoring group was prepared and systematically investigated.

The synthetic approach to sensitizer FNE53 is depicted in Scheme 1. The synthesis of the key core, 8,11-dibromodithieno[2,3-*a*:3′,2′-*c*]phenazine (**5**),[43] by direct oxidation ring-closure of 5,8-dibromo-2,3-di(thien-2-yl)-quinoxaline[32] is not applicable because of their similar polarities, and it is not successful to separate the product. An alternative straightforward approach is to begin with 3,3′-bithiophene (**1**) which can be easily converted to benzo[1,2-*b*:4,3-*b*′]dithiophene-4,5-dione (**2**)[44] by refluxing with oxalyl dichloride in 1,2-dichloroethane with a yield of 68%. Then, a ring-closure reaction was carried out by condensation with 3,6-dibromobenzene-1,2-diamine (**4**)[45] obtained by reduction of 4,7-dibromobenzo[*c*][1,2,5]thiadiazole (**3**) with sodium borohydride in refluxing ethanol solution using acetic acid as catalyst. Then, intermediate compound **7** was obtained via a Stille coupling[46] between bromide **5** and stannane **6**.[47] After refluxing with a Vilsmeier reagent,[48] the corresponding monoaldehyde-substituted derivative **8** was produced. In the last step, the obtained precursor was converted to the target sensitizer FNE53 by Knövenagel condensation[49] with cyanoacetic acid through refluxing acetonitrile in the presence of piperidine. The chemical structure of the resulting sensitizer was verified by ^{1}H NMR, ^{13}C NMR, and mass spectroscopy. The obtained NIR dye is black in the solid state and can freely

Chart 2. Chemical Structures of Sensitizers FNE48, FNE53, and FNE46

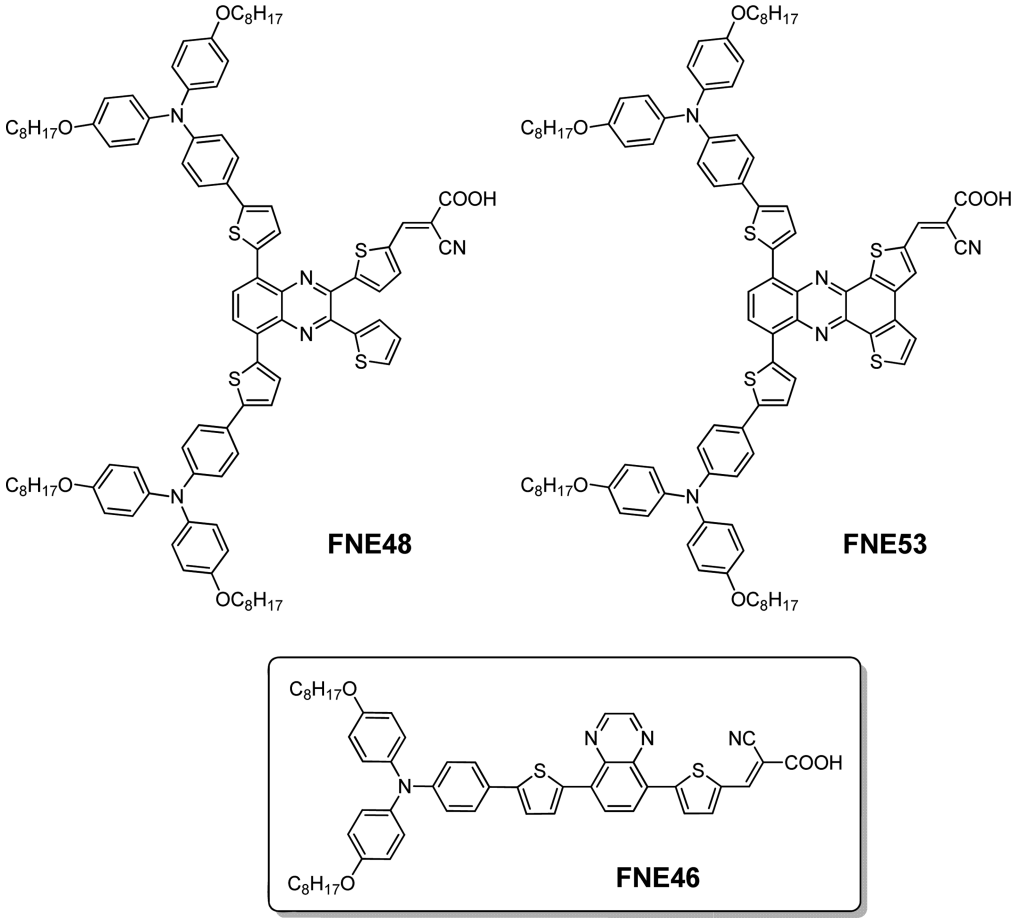

dissolve in dichloromethane (DCM), tetrahydrofuran (THF), or toluene to produce a deep green solution.

UV–Vis Absorption Properties. The electronic absorption spectra of sensitizers FNE53, FNE46, and FNE48 in toluene solutions are shown in Figure 1, and the data are summarized in Table 1. Similar to sensitizers FNE46 and FNE48, the NIR dye FNE53 exhibits two distinct absorption bands. The absorption band below 500 nm corresponds to the $\pi-\pi^*$ electron transitions of the conjugated backbone, while the other one in the lower energy region can be assigned to the ICT interactions[50] between the electron donating moiety and the electron-withdrawing moiety.[51] As shown in Figure 1, the UV–vis absorption spectrum of sensitizer FNE53 displays an ICT band at 629 nm, which is bathochromically shifted by 87 nm in comparison to that of sensitizer FNE48 (542 nm). This is due to the replacement of the twisted 2,3-di(thien-2-yl)quinoxaline unit in FNE48 by a coplanar dithieno[2,3-*a*:3′,2′-*c*]phenazine core in FNE53, which results in the better π-conjugation and facile ICT. Under the same conditions, FNE46 exhibits an ICT band at 520 nm. Importantly, this absorption band can well compensate for the valley in that region of the UV spectrum based on sensitizer FNE53. Therefore, organic dye FNE46 is an ideal co-adsorbent in the DSSC based on the NIR sensitizer FNE53 to recover the dip in the absorption spectrum.

When sensitizer FNE53 was adsorbed onto a mesoporous TiO_2 film, the absorption spectrum covers the whole visible region and extends to the NIR region with the maximum at 621 nm (Figure 2), which is greatly beneficial for solar light harvesting. In comparison to the ICT band for FNE48 at 536 nm, a simple fusion of the two thiophene rings on the pyrazine derivative successfully bathochromically shifts the ICT band by 85 nm without further structural modification. Compared with the absorption spectrum in toluene solution, the ICT band for sensitizer FNE53 on TiO_2 film hypsochomically shifts to 621 nm by only 8 nm, which is due to the deprotonation of the carboxylic acid.[31,32,52] However, the hypsochromic shift is much smaller than those for D–π–*A* featured organic dyes,[53] resulting from the incorporation of the auxiliary dithieno[2,3-*a*:3′,2′-*c*]phenazine acceptor. After anchoring sensitizer onto TiO_2 surface, although the anchoring group is deprotonated, the ICT from the electron donor to the inserted dithieno[2,3-*a*:3′,2′-*c*]phenazine unit is not weakened significantly, and therefore, only a slight hypsochromic shift can be observed. This phenomenon is similar to the comparative sensitizers FNE46 and FNE48 for which a hypsochromic shift of only 26 and 6 nm, respectively, can be observed between the spectra in toluene solution and on titania film. The different hypsochromic shifts for the absorption maxima are probably due to their different deprotonation effect. Although sensitizers FNE46 and FNE48 contain the same electron-donating and electron-withdrawing groups, for sensitizer FNE46, the donor and acceptor are linearly linked, resulting in a better conjugation. Therefore, the deprotonation of the carboxylic acid may have a more significant effect on the absorption maximum shift for sensitizer FNE46 as compared to that of FNE48, which contains a twisted conjugation structure. Moreover, the absorption intensity for FNE53 on TiO_2 film is relatively

Scheme 1. Synthetic Route for Sensitizer FNE53

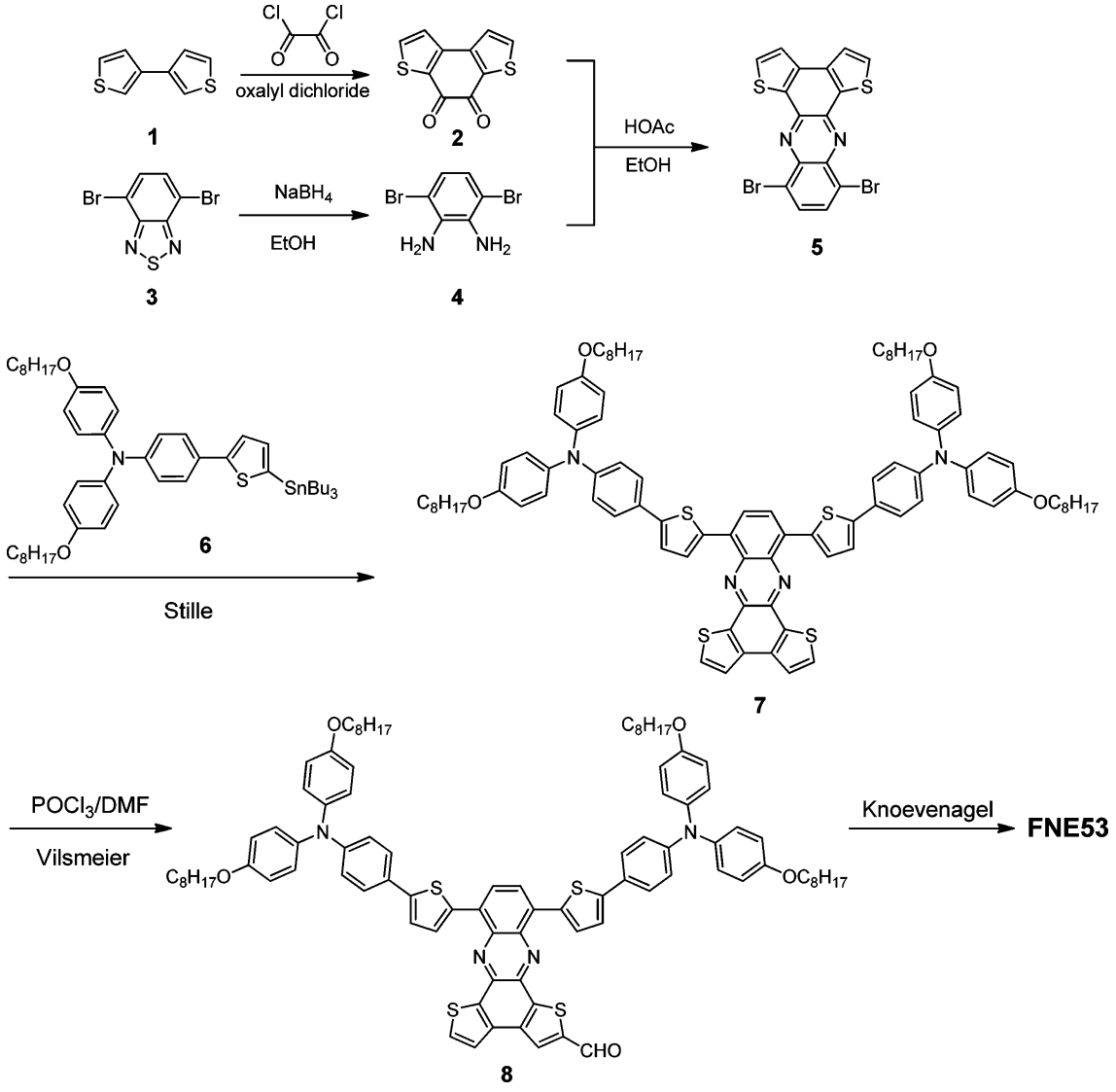

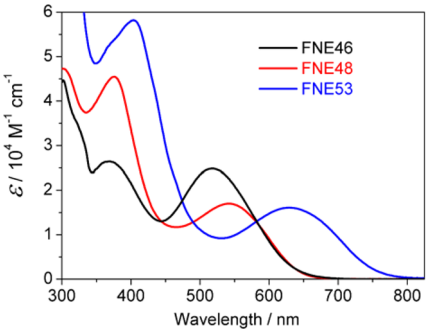

Figure 1. UV−vis absorption spectra of sensitizers FNE46, FNE48, and FNE53 in toluene solutions.

Table 1. UV−Vis Absorption and Electrochemical Properties of Sensitizers FNE46, FNE48, and FNE53

dye	λ_{max} (nm)[a]	ε (M^{-1} cm^{-1})[a]	λ_{max} on TiO_2 (nm)	HOMO (V)[b]	E_{0-0} (eV)	LUMO (V)[b]
FNE48	542	1.7×10^4	536	0.81	1.84	−1.03
FNE53	629	1.6×10^4	621	0.86	1.60	−0.74
FNE46	520	2.5×10^4	494	0.88	1.93	−1.05

[a]Absorption peaks (λ_{max}) and molar extinction coefficients (ε) were measured in toluene solutions (~10^{-5} M). [b]The potentials (vs NHE, the same below) were calibrated with ferrocene.

lower than those for FNE48 and FNE46, which stems from the reduced dye adsorption amount on the TiO_2 surface. Under the same conditions, the surface concentration is 1.56×10^{-8} mol cm^{-2} μm^{-1} for sensitizer FNE46 and 0.77×10^{-8} mol cm^{-2} μm^{-1} for sensitizer FNE48, while that of FNE53 significantly decreases to 0.43×10^{-8} mol cm^{-2} μm^{-1}. Therefore, when cocktail dyes of FNE46 and FNE53 were coadsorbed on TiO_2 film, the absorption spectra exhibit a major absorption band around 500 nm and a weak shoulder around 670 nm.

Electrochemical Properties. Cyclic voltammetry (CV) was employed to investigate the electrochemical properties of sensitizer FNE53 (Figure S1, Supporting Information). The first oxidation potential, which corresponds to the HOMO level of sensitizer FNE53, is determined to be 0.86 V (vs NHE, the same below). Under the same condition, sensitizer FNE46 displays a HOMO level at 0.88 V, which is similar to that for sensitizer FNE53 and originates from the fact that both

dx.doi.org/10.1021/am505153q | ACS Appl. Mater. Interfaces 2014, 6, 19308−19317

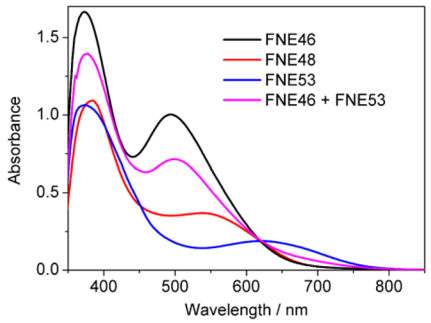

Figure 2. UV–vis absorption spectra of sensitizers FNE46, FNE48, and FNE53 on TiO_2 films.

sensitizers consist of the same donor unit. The HOMO levels are more positive than the redox potential of the I^-/I_3^- redox couple (~0.4 V), suggesting that the oxidized organic dyes can be thermodynamically regenerated during the operation.[54] Estimated from eq 1:[55]

$$E_{LUMO} = E_{HOMO} - E_g^{opt} \quad (1)$$

where E_g^{opt} is the optical band gap derived from the wavelength at 10% maximum absorption intensity for the dye-loaded TiO_2 film,[56] the LUMO levels of dyes FNE53 and FNE46 are calculated to be −0.74 and −1.05 V, respectively. As compared with sensitizer FNE46 with quinoxaline moiety, sensitizer FNE53 containing dithieno[2,3-*a*:3′,2′-*c*]phenazine unit has downward shifted the LUMO level from −1.05 to −0.74 V. This indicates that the dithieno[2,3-*a*:3′,2′-*c*]phenazine unit has a much stronger electron withdrawing ability as compared to the quinoxaline unit. However, the positively shifted LUMO level resulted in a decreased driving force for electron injection from the excited state of the organic sensitizers to the TiO_2 films.

Molecular Orbital Calculations. To investigate the geometrical and electronic properties of the NIR sensitizer FNE53, density functional calculations were conducted using the Gaussian 03 program package at the B3LYP/6-31G(d) level.[57] The frontier molecular orbitals (Figure S2, Supporting Information) revealed that the HOMO is distributed along the double D-π system, whereas the LUMO is evenly delocalized across the dithieno[2,3-*a*:3′,2′-*c*]phenazine and cyanoacrylic acid units. The overlapping distribution of the HOMO and LUMO orbitals on the dithieno[2,3-*a*:3′,2′-*c*]phenazine unit indirectly suggests that the dithieno[2,3-*a*:3′,2′-*c*]phenazine unit facilitates the electron transfer from the triarylamine donor to the anchor group (i.e., cyanoacrylic acid unit).

Solar Cell Performance. Quasi-solid-state DSSCs based on FNE53 and FNE46 were fabricated using a quasi-solid-state gel electrolyte containing 0.1 M LiI, 0.1 M I_2, 0.1 M 4-*tert*-butylpyridine (TBP), 0.6 M 1,2-dimethyl-3-propylimidazolium iodide (DMPImI), and 5 wt % poly(vinylidenefluoride-*co*-hexafluoropropylene) in 3-methoxypropionitrile (MPN). The current density–voltage (J–V) curves measured under 100 mW cm^{-2} simulated AM1.5G solar light are shown in Figure 3a and the detailed photovoltaic parameters are presented in Table 2. Sensitizer FNE53 based quasi-solid-state DSSC produced a J_{sc} of 13.45 mA cm^{-2}, a V_{oc} of 604 mV, and a fill factor (FF) of 0.65, respectively, corresponding to an efficiency (η) of 5.28%. Although sensitizer FNE53 exhibited a broader absorption spectrum extending to the NIR region, the relatively poor DSSC performance is probably due to the low photogenerated

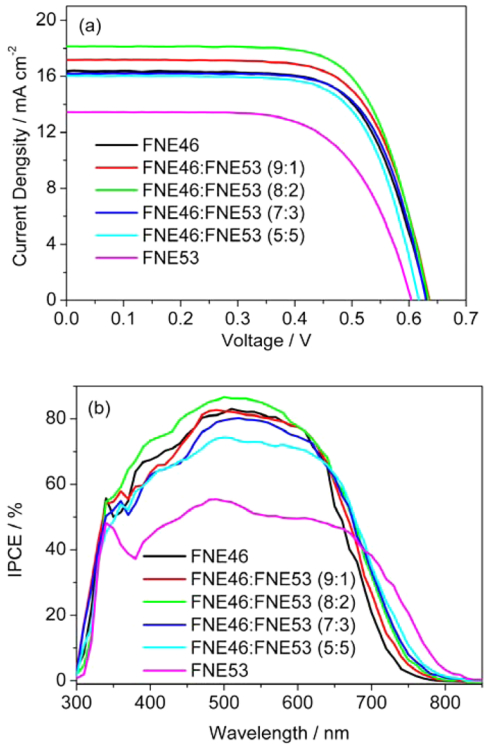

Figure 3. (a) J–V curves and (b) IPCE spectra for FNE46, FNE53, and their cosensitized quasi-solid-state DSSCs.

Table 2. Photovoltaic Parameters of the Cocktail-Type Quasi-Solid-State DSSCs based on Sensitizers FNE46 and FNE53 with Different Ratios

DSSC	molar ratio of FNE46/FNE53	V_{oc} (mV)	J_{sc} (mA cm^{-2})	FF (%)	η (%)
1	10:0	631 ± 2	16.38 ± 0.26	69 ± 1	7.03 ± 0.10
2	9:1	636 ± 4	17.18 ± 0.11	69 ± 1	7.46 ± 0.08
3	8:2	634 ± 5	18.12 ± 0.17	70 ± 1	8.00 ± 0.04
4	7:3	630 ± 5	16.20 ± 0.22	70 ± 1	6.98 ± 0.16
5	5:5	617 ± 8	16.01 ± 0.31	70 ± 1	6.70 ± 0.21
6	0:10	604 ± 3	13.45 ± 0.13	65 ± 1	5.19 ± 0.09

current induced by the weaker driving force for the electron injection from the excited organic dyes into the TiO_2 film.

To fully utilize the advantage of panchromatic light harvesting property for sensitizer FNE53, cocktail-type quasi-solid-state DSSCs cosensitized by FNE46 and FNE53 were fabricated sine these two metal-free organic sensitizers have complementary absorption properties. The cosensitized working electrolytes were constructed by immersing TiO_2 films in a toluene solution containing sensitizers FNE53 and FNE46 at room temperature for complete dye adsorption. To achieve the best DSSC performance, we optimized the molar ratio between cosensitizers FNE53 and FNE46, and the performance data are summarized in Table 2. As shown in Figure 3a, the cosensitized quasi-solid-state DSSC based on sensitizers FNE46 and FNE53 with a molar ratio of 8:2 achieved the best DSSC performance, which provided a J_{sc} of 18.12 mA cm^{-2}, a V_{oc} of 634 mV, and an FF of 0.70, respectively, corresponding to an η of 8.04%. This performance was substantially better than that of the DSSC based on FNE46 alone (Table 2). The J_{sc} value increased from 16.38 mA cm^{-2} for FNE46-based DSSC to 18.12 mA cm^{-2} for

dx.doi.org/10.1021/am505153q | ACS Appl. Mater. Interfaces 2014, 6, 19308–19317

the cocktail-type quasi-solid-state DSSC; meanwhile, the V_{oc} and FF values remained about the same, and consequently, the overall conversion efficiency was improved by 13%. These results indicate that the ratio of cocktail dyes loaded on the TiO_2 films has significant effect on the performance of the cosensitized DSSCs.

To understand the different J_{sc} values, action spectra of the incident photon-to-current conversion efficiencies as a function of incident wavelength for the quasi-solid-state DSSCs are recorded and shown in Figure 3b. The quasi-solid-state DSSC based on sensitizer FNE53 alone exhibits much broader IPCE spectrum covering the whole visible region and partial NIR region with the threshold over 850 nm, which is much broader than that for the DSSC based on FNE46 and consistent with their absorption spectra. However, the maximum IPCE value for DSSC based on the sensitizer FNE53 is much lower than that for FNE46, which is in good agreement with the tendency of the LUMO levels for the corresponding organic dyes. A more positive LUMO level may induce an insufficient electron injection driving force, which resulted in a lower IPCE value. As shown in Figure 3b, when the content of FNE53 increased, the IPCE response region continuously widened due to the wider photo response region of sensitizer FNE53. While the maximum IPCE value first increased slightly when the content ratio of FNE46/FNE53 changed from 10:0 to 9:1, and further to 8:2, which may be due to reduced electron loss from charge recombination. However, upon further increasing FNE53 content, the maximum IPCE value dramatically decreased, probably due to the reduced dye loading amount on the TiO_2 films.

The other key performance parameter, V_{oc}, is related to the conduction band position of TiO_2 and the charge recombination rate in quasi-solid-state DSSCs.[58] To understand the difference V_{oc} values for the resulting quasi-solid-state DSSCs, the CB position of the dye-loaded TiO_2 films were investigated through charge extraction and intensity modulated photovoltage spectroscopy (IMVS) measurements.[59] According to the method developed by Frank and co-workers,[60] the movement of CB contributed to the change in V_{oc} at constant photoinduced charge density (Q), which was measured with charge extraction technique under illumination of a white light from LED.[61] A higher V_{oc} at constant Q indicates an upward (or negative) shift of the CB edge, and vice versa. Figure 4 shows the relation between V_{oc} and Q at open circuit for the quasi-solid-state DSSCs. It can be found that for quasi-solid-state DSSCs sensitized with FNE53 or FNE46 alone, or cosensitized with FNE53 and FNE46, the V_{oc} increases linearly

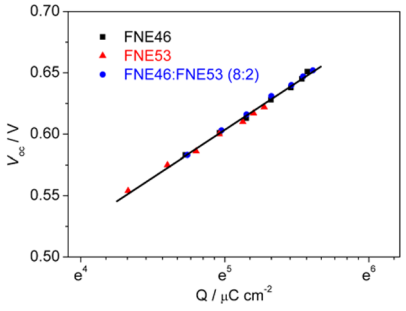

Figure 4. Charge density at open circuit as a function of V_{oc} for the quasi-solid-state DSSCs.

with the logarithm of Q, and all the curves have almost identical slope (78 mV) according to eq 2:[59]

$$V_{oc} \propto m_c \ln(n) \tag{2}$$

where n is the electron density. At fixed Q, the same V_{oc} values for all the DSSCs indicates that the cosensitizer has no influence on the movement of TiO_2 conduction band.

Although the NIR sensitizer FNE53-based DSSC produced a very promising V_{oc} value for the quasi-solid state DSSCs based on organic NIR dyes, it can still be found that the V_{oc} value increased from 604 mV for FNE53-sensitized DSSC to 631 mV for FNE46-based DSSC, and further to 634 mV for FNE53/FNE46-cosensitized DSSC. This should be attributed to the repression of charge recombination, which is related to electron lifetime (τ).[62] The electron lifetime was measured by IMVS and obtained from the frequency at the top of the semicircle (f_{min}) according to eq 3:[59]

$$\tau = (2\pi f_{min})^{-1} \tag{3}$$

Figure 5 shows the electron lifetime as a function of charge density at open circuit. The electron lifetime for a certain DSSC

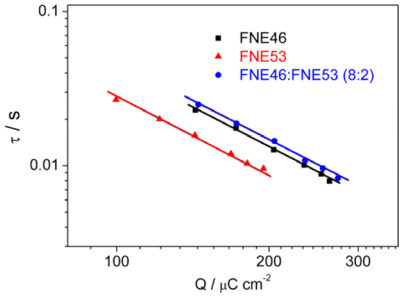

Figure 5. Electron lifetime as a function of charge density at open circuit for the quasi-solid-state DSSCs.

decreases with charge density following a power law relation with the same slope, suggesting the same charge recombination mechanism in the three quasi-solid-state DSSCs. At a fixed charge density, the electron lifetime for the quasi-solid-state DSSCs sensitized with FNE46 or cosensitized with FNE53 and FNE46 is larger than that of FNE53-based DSSC by around 1.6-fold. This suggests that the charge recombination between electrons in TiO_2 film and electron acceptors in the electrolyte is reduced. Therefore, more charge is accumulated in TiO_2, and the Fermi level moves upward, resulting in a larger V_{oc} value. V_{oc} solely originated from the suppression of charge recombination varies as electron density (n) or charge density (Q) changes, which follows eq 4:[59]

$$\Delta V_{oc} = m_c \ln \frac{n_2}{n_1} = m_c \ln \frac{Q_2}{Q_1} \tag{4}$$

Under 100 W m^{-2} white LED light, the extracted charge densities are 181, 254, and 256 μC cm^{-2} for FNE46, FNE53, and their cosensitized DSSCs, respectively. According to eq 4, the V_{oc} gain from FNE53 sensitized DSSC to FNE46 sensitized DSSC or to their cosensitized DSSC is calculated to be 26 and 27 mV, respectively, which is in good agreement with the experimentally observed V_{oc} enhancement (27 and 30 mV, respectively) for the corresponding quasi-solid-state DSSCs.

For future practical applications, it is quite important for DSSC devices to achieve a long lifetime. Because quasi-solid-

state gel electrolytes[24] are not flowing or volatile, the related quasi-solid-state DSSCs have shown much better stability. To investigate the stability of the resulting cosensitized quasi-solid-state DSSC, the photovoltaic performance parameters of the cosensitized quasi-solid-state DSSC are evaluated under one sun soaking and the date are shown in Figure 6. It can be found

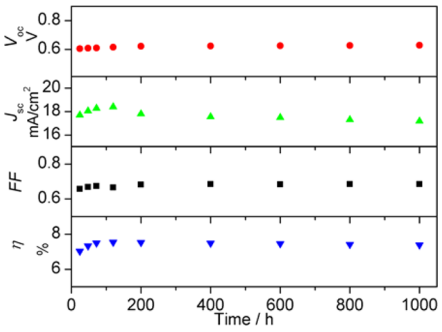

Figure 6. Evolutions of photovoltaic performance parameters for quasi-solid-state DSSC cosensitized with FNE46 and FNE53 under one sun soaking.

that the J_{sc}, V_{oc}, and FF values slightly changed within 5%. And most importantly, the power conversion efficiency remained 98% of the initial value after 1000 h of one sun soaking, which indicates that the quasi-solid-state DSSCs based on the cosensitizers demonstrate good long-term stability.

CONCLUSIONS

In summary, a novel NIR organic sensitizer FNE53 containing a strong electron-withdrawing unit, dithieno[2,3-*a*:3′,2′-*c*]-phenazine, has been designed and synthesized. The absorption spectrum of sensitizer FNE53 covers the whole visible region and extends to the NIR region, which exhibits complementary absorption profile to another quinoxaline-based organic dye FNE46. When FNE46 and FNE53 were used as cosensitizers for metal-free cocktail-type quasi-solid-state DSSCs, the DSSC exhibited a much higher IPCE value compared to that of the DSSC based on sensitizer FNE53 and broader IPCE response in comparison to that of the DSSC based on sensitizer FNE46, respectively. By optimizing the molar ratio between the two cocktail dyes, a highest energy conversion efficiency of 8.04% was achieved in a cocktail-type quasi-solid-state DSSC cosensitized with FNE46 and FNE53, which also exhibited good long-term stability after continuous light soaking for 1000 h.

EXPERIMENTAL SECTION

Materials and Reagents. 3-Bromothiophene, benzothiadiazole, oxalyl chloride, and cyanoacetic acid were purchased from J&K Chemical, Ltd. (Beijing, China). Organic solvents were purified using the standard process. Other chemicals were used as received from commercial sources without further purification. Transparent conductive glass (F-doped SnO_2, FTO, 15 Ω/square, transmittance of 80%, Nippon Sheet Glass Co., Japan) was used as the substrate for the fabrication of TiO_2 thin film electrode.

Synthesis. The synthetic route of the sensitizer FNE53 is shown in Scheme 1. Compounds **2**,[39] **4**,[45] **5**,[43] and **6**[47] were synthesized according to the procedure in the literature.

Synthesis of Compound 7. Under a nitrogen atmosphere, a mixture of compound **5** (350 mg, 0.78 mmol), compound **6** (2.04 g, 2.33 mmol), and $Pd(PPh_3)_2Cl_2$ (50 mg, 0.07 mmol) in *N*,*N*-dimethylformamide (DMF, 30 mL) was stirred and heated at 90 °C for 15 h. After the solvent was evaporated, the crude product was purified by flash column chromatography (silica gel, DCM/PE = 1:2). Black solid **7** was obtained with a yield of 58% (650 mg). ^{1}H NMR (400 MHz, THF-d_8, δ): 8.06 (s, 2H), 7.85−7.83 (d, 2H, J = 5.0 Hz), 7.75 (s, 2H), 7.67−7.66 (d, 2H, J = 5.0 Hz), 7.54−7.52 (d, 4H, J = 7.7 Hz), 7.17 (s, 2H), 6.99−6.97 (d, 8H, J = 7.7 Hz), 6.85−6.84 (d, 4H, J = 7.6 Hz), 6.78−6.76 (d, 8H, J = 7.4 Hz), 3.85 (t, 8H, J = 6.0 Hz), 1.71−1.64 (m, 8H), 1.40−1.36 (m, 8H), 1.26−1.22 (m, 32H), 0.82−0.79 (m, 12H). ^{13}C NMR (100 MHz, THF-d_8, δ): 157.9, 150.2, 149.4, 142.7, 139.3, 138.9, 138.6, 137.1, 133.1, 131.9, 129.3, 128.7, 128.5, 127.9, 126.72, 126.69, 124.8, 122.8, 122.4, 117.1, 69.9, 34.0, 31.57, 31.55, 31.5, 28.3, 24.7, 15.7.

Synthesis of Compound 8. Under a nitrogen atmosphere, compound **7** (300 mg, 0.21 mmol) and DMF (24 mg, 0.33 mmol) were dissolved in 30 mL of chloroform ($CHCl_3$). To this solution, phosphorus oxychloride (64 mg, 0.42 mmol) was added slowly. The mixture was stirred for 20 min at room temperature and then heated to 80 °C for 12 h. After cooling to room temperature, 60 mL saturated sodium acetate solution was added to the green reaction solution and stirred for 30 min. The mixture was poured into ice water (50 mL) and neutralized (pH = 7) through the addition of sodium hydroxide solution. The product was extracted with DCM three times. The combined organic solution was washed with sodium bicarbonate and brine and dried over anhydrous sodium sulfate. After the solvent was removed, the residue was purified by flash column chromatography (silica gel, DCM/PE = 1:1). Black solid **8** was obtained with a yield of 42% (130 mg). ^{1}H NMR (400 MHz, THF-d_8, δ): 9.72 (s, 1H), 7.73−7.70 (m, 2H), 7.63−7.61 (s, 1H, J = 8.0 Hz), 7.56−7.54 (d, 1H, J = 4.9 Hz), 7.51−7.50 (d, 1H, J = 4.8 Hz), 7.40−7.36 (m, 3H), 7.30−7.28 (d, 2H, J = 4.9 Hz), 7.25−7.23 (d, 2H, J = 8.3 Hz), 7.02−6.93 (m, 9H), 6.84−6.76 (m, 12H), 3.87−3.84 (m, 8H), 1.72−1.65 (m, 8H), 1.41−1.39 (m, 8H), 1.27−1.18 (m, 32H), 0.81−0.80 (m, 12H). ^{13}C NMR (100 MHz, THF-d_8, δ): 186.6, 159.6, 158.4, 157.9, 151.7, 150.1, 149.7, 142.7, 142.0, 139.1, 139.0, 138.9, 138.74, 138.72, 138.69, 138.3, 138.1, 137.0, 136.9, 136.6, 133.1, 132.7, 132.5, 131.62, 131.61, 130.3, 129.3, 129.2, 128.8, 128.7, 127.9, 127.3, 126.3, 125.7, 125.5, 124.6, 122.7, 122.3, 120.9, 117.3, 117.1, 69.9, 34.0, 31.6, 31.54, 31.47, 28.3, 24.7, 15.7.

Synthesis of FNE53. Under a nitrogen atmosphere, a mixture of compound **8** (80 mg, 0.05 mmol) and cyanoacetic acid (14 mg, 0.16 mmol) in a solution of acetonitrile (6 mL) and $CHCl_3$ (6 mL) was refluxed in the presence of piperidine (0.05 mL) for 8 h. After cooling to room temperature, poured into water and extracted with DCM, the combined organic solution was washed with brine and dried over anhydrous sodium sulfate. After the solvent was evaporated, the crude product was purified by flash column chromatography (silica gel, DCM/MeOH = 10:1). Black solid FNE53 was obtained with a yield of 77% (65 mg). ^{1}H NMR (400 MHz, THF-d_8, δ): 8.47 (s, 1H), 8.21 (s, 1H), 7.77−7.57 (m, 4H), 7.37−7.27 (m, 7H), 7.00−6.98 (m, 9H), 6.79−6.77 (m, 12H), 3.89−3.81 (m, 8H), 1.72−1.67 (m, 8H), 1.42−1.40 (m, 8H), 1.29−1.14 (m, 32H), 0.81−0.72 (m, 12H). ^{13}C NMR (100 MHz, THF-d_8, δ): 156.6, 156.5, 156.0, 148.4, 148.3, 147.8, 140.9, 140.3, 137.3, 137.1, 137.04, 136.98, 136.9, 135.2, 134.7, 130.7, 130.6, 129.7, 127.7, 127.6, 127.5, 126.7, 126.1, 123.1, 120.58, 120.56, 118.9, 115.4, 115.3, 68.1, 32.1, 29.8, 29.7, 29.5, 26.4, 22.8, 13.7. Elemental analysis: calcd for $C_{96}H_{103}N_5O_6S_4$ (%), C, 74.33; H, 6.69; N, 4.51; found, C, 71.86; H, 6.94; N, 4.32. HRMS (ESI, m/z): calcd for $C_{96}H_{102}N_5O_6S_4$ [$(M - H)^-$], 1549.6746; found, 1549.6717.

Characterizations. UV−vis absorption spectra of dye solutions and dye-loaded films were measured using a Shimadzu UV-2550PC spectrometer. The film thickness was measured with a surface profiler (Veeco Dektak 150). CV measurements were carried out with a CHI660E electrochemical workstation using a typical three-electrode electrochemical cell in a 0.1 M solution of tetrabutylammonium hexafluorophosphate in dry acetonitrile with a scan rate of 50 mV/s^{-1}. Dye-adsorbed TiO_2 on conductive glass was used as the working electrode, a Pt wire was used as the counter electrode, and an Ag/Ag^+ electrode was used as the reference electrode. The potential of the reference electrode was calibrated by ferrocene, and all potentials mentioned in this work are against normal hydrogen electrode (NHE).

DSSC Fabrication and Photovoltaic Measurements. The quasi-solid-state DSSCs were fabricated according to our previously reported methods.[31,63] The current density−voltage (J−V) characteristics of the DSSCs were measured using a Keithley 2400 source meter under the illumination of AM1.5G simulated solar light (Oriel-91193 equipped with a 1000 W Xe lamp and an AM1.5 filter). The incident light intensity was calibrated with a standard silicon solar cell (Newport 91150). IMVS analysis and charge extraction were carried out on an electrochemical workstation (Zahner XPOT, Germany). The intensity modulated spectra were measured at room temperature with white light intensity ranging from 20 to 120 W m^{-2}, in modulation frequency ranging from 0.1 Hz to 10 kHz, and with modulation amplitude less than 5% of the light intensity. Action spectra of the incident monochromatic photon-to-electron conversion efficiency (IPCE) for the solar cells were obtained with an Oriel-74125 system (Oriel Instruments).

■ ASSOCIATED CONTENT

Ⓢ Supporting Information

Cyclic voltammograms of the dye-loaded TiO_2 films and the frontier molecular orbitals of the target NIR dye. This material is available free of charge via the Internet at http://pubs.acs.org.

■ AUTHOR INFORMATION

Corresponding Author

*E-mail: zhougang@fudan.edu.cn. Tel: +86-21-5163-0350. Fax: +86-21-5163-0345.

Notes

The authors declare no competing financial interest.

■ ACKNOWLEDGMENTS

This work was financially supported by the National Basic Research Program of China (2011CB933302), the National Natural Science Foundation of China (51273045), NCET-12-0122, STCSM (12JC1401500), the Shanghai Leading Academic Discipline Project (B108), and the Jiangsu Major Program (BY2010147).

■ REFERENCES

(1) O'Regan, B.; Grätzel, M. A Low-Cost, High-Efficiency Solar Cell Based on Dye-Sensitized Colloidal TiO_2 Films. *Nature* **1991**, *353*, 737−740.

(2) Wu, W.-Q.; Feng, H.-L.; Rao, H.-S.; Xu, Y.-F; Kuang, D.-B.; Su, C.-Y. Maximizing Omnidirectional Light Harvesting in Metal Oxide Hyperbranched Array Architectures. *Nat. Commun.* **2014**, *5*, 3968−3971.

(3) Wu, W.-Q.; Xu, Y.-F.; Rao, H.-S.; Su, C.-Y.; Kuang, D.-B. Multistack Integration of Three-Dimensional Hyperbranched Anatase Titania Architectures for High-Efficiency Dye-Sensitized Solar Cells. *J. Am. Chem. Soc.* **2014**, *136*, 6437−6445.

(4) Wu, W.-Q.; Xu, Y.-F.; Rao, H.-S.; Feng, H.-L.; Su, C.-Y.; Kuang, D.-B. Constructing 3D Branched Nanowire Coated Macroporous Metal Oxide Electrodes with Homogeneous or Heterogeneous Compositions for Efficient Solar Cells. *Angew. Chem., Int. Ed.* **2014**, *53*, 4816−4821.

(5) Qin, C.; Numata, Y.; Zhang, S.; Yang, X.; Islam, A.; Zhang, K.; Chen, H.; Han, L. Novel Near-Infrared Squaraine Sensitizers for Stable and Efficient Dye-Sensitized Solar Cells. *Adv. Funct. Mater.* **2014**, *24*, 3059−3066.

(6) Yella, A.; Mai, C.-L.; Zakeeruddin, S. M.; Chang, S.-N.; Hsieh, C.-H.; Yeh, C.-Y.; Grätzel, M. Molecular Engineering of Push-Pull Porphyrin Dyes for Highly Efficient Dye-Sensitized Solar Cells: The Role of Benzene Spacers. *Angew. Chem., Int. Ed.* **2014**, *53*, 2973−2977.

(7) Geiger, T.; Kuster, S.; Yum, J. H.; Moon, S. J.; Nazeeruddin, M. K.; Grätzel, M.; Nüesch, F. Molecular Design of Unsymmetrical Squaraine Dyes for High Efficiency Conversion of Low Energy Photons into Electrons Using TiO_2 Nanocrystalline Films. *Adv. Funct. Mater.* **2009**, *19*, 2720−2727.

(8) Tian, H.; Yang, X.; Chen, R.; Hagfeldt, A.; Sun, L. A Metal-Free "Black Dye" for Panchromatic Dye-Sensitized Solar Cells. *Energy Environ. Sci.* **2009**, *2*, 674−677.

(9) Edvinsson, T.; Li, C.; Pschirer, N.; Schoneboom, J.; Eickemeyer, F.; Sens, R.; Boschloo, G.; Herrmann, A.; Müllen, K.; Hagfeldt, A. Intramolecular Charge-Transfer Tuning of Perylenes: Spectroscopic Features and Performance in Dye-Sensitized Solar Cells. *J. Phys. Chem. C* **2007**, *111*, 15137−15140.

(10) Erten-Ela, S.; Yilmaz, M. Z.; Icli, B.; Dede, Y.; Icli, S.; Akkaya, E. U. A Panchromatic Boradiazaindacene (BODIPY) Sensitizer for Dye-Sensitized Solar Cells. *Org. Lett.* **2008**, *10*, 3299−3302.

(11) He, J.; Hagfeldt, A.; Lindquist, S.-E.; Grennberg, H.; Korodi, F.; Sun, L.; Åkermark, B. Phthalocyanine-Sensitized Nanostructured TiO_2 Electrodes Prepared by a Novel Anchoring Method. *Langmuir* **2001**, *17*, 2743−2747.

(12) Hao, Y.; Yang, X.; Cong, J.; Tian, H.; Hagfeldt, A.; Sun, L. Efficient Near Infrared D−π−A Sensitizers with Lateral Anchoring Group for Dye-Sensitized Solar Cells. *Chem. Commun.* **2009**, *45*, 4031−4033.

(13) Qu, S.; Wu, W.; Hua, J.; Kong, C.; Long, Y.; Tian, H. New Diketopyrrolopyrrole (DPP) Dyes for Efficient Dye-Sensitized Solar Cells. *J. Phys. Chem. C* **2010**, *114*, 1343−1349.

(14) Lu, X.; Zhou, G.; Wang, H.; Feng, Q.; Wang, Z.-S. Near Infrared Thieno[3,4-*b*]pyrazine Sensitizers For Efficient Quasi-Solid-State Dye-Sensitized Solar Cells. *Phys. Chem. Chem. Phys.* **2012**, *14*, 4802−4809.

(15) Jiao, C.; Zu, N.; Huang, K.-W.; Wang, P.; Wu, J. Perylene Anhydride Fused Porphyrins as Near-Infrared Sensitizers for Dye-Sensitized Solar Cells. *Org. Lett.* **2011**, *13*, 3652−3655.

(16) Qin, C.; Numata, Y.; Zhang, S.; Islam, A.; Yang, X.; Sodeyama, K.; Tateyama, Y.; Han, L. A Near-Infrared *cis*-Configured Squaraine Co-Sensitizer for High-Efficiency Dye-Sensitized Solar Cells. *Adv. Funct. Mater.* **2013**, *23*, 3782−3789.

(17) Yum, J.-H.; Baranoff, E.; Wenger, S.; Nazeeruddin, M. K.; Grätzel, M. Panchromatic Engineering for Dye-Sensitized Solar Cells. *Energy Environ. Sci.* **2011**, *4*, 842−857.

(18) Yella, A.; Lee, H.-W.; Tsao, H. N.; Yi, C.; Chandiran, A. K.; Nazeeruddin, M. K.; Diau, E. W.-G.; Yeh, C.-Y.; Zakeeruddin, S. M.; Grätzel, M. Porphyrin-Sensitized Solar Cells with Cobalt (II/III)-Based Redox Electrolyte Exceed 12% Efficiency. *Science* **2011**, *334*, 629−634.

(19) Kimura, M.; Nomoto, H.; Masaki, N.; Mori, S. Dye Molecules for Simple Co-Sensitization Process: Fabrication of Mixed-Dye-Sensitized Solar Cells. *Angew. Chem., Int. Ed.* **2012**, *51*, 4371−4374.

(20) Wang, Y.; Chen, B.; Wu, W.; Li, X.; Zhu, W.; Tian, H.; Xie, Y. Efficient Solar Cells Sensitized by Porphyrins with an Extended Conjugation Framework and a Carbazole Donor: From Molecular Design to Cosensitization. *Angew. Chem., Int. Ed.* **2014**, *53*, 10779−10783.

(21) Li, L.-L.; Diau, E. W.-G. Porphyrin-Sensitized Solar Cells. *Chem. Soc. Rev.* **2013**, *42*, 291−304.

(22) Mishra, A.; Fischer, M. K. R.; Bäuerle, P. Metal-Free Organic Dyes for Dye-Sensitized Solar Cells: From Structure: Property Relationships to Design Rules. *Angew. Chem., Int. Ed.* **2009**, *48*, 2474−2499.

(23) Zhang, M.; Wang, Y.; Xu, M.; Ma, W.; Li, R.; Wang, P. Design of High-Efficiency Organic Dyes for Titania Solar Cells Based on the Chromophoric Core of Cyclopentadithiophene-Benzothiadiazole. *Energy Environ. Sci.* **2013**, *6*, 2944−2949.

(24) Wang, P.; Zakeeruddin, S. M.; Moser, J. E.; Nazeeruddin, M. K.; Sekiguchi, T.; Grätzel, M. A Stable Quasi-Solid-State Dye-Sensitized Solar Cell with an Amphiphilic Ruthenium Sensitizer and Polymer Gel Electrolyte. *Nat. Mater.* **2003**, *2*, 402−407.

(25) Chang, D. W.; Lee, H. J.; Kim, J. H.; Park, S. Y.; Park, S.-M.; Dai, L.; Baek, J.-B. Novel Quinoxaline-Based Organic Sensitizers for Dye-Sensitized Solar Cells. *Org. Lett.* **2011**, *13*, 3880−3883.

(26) Pei, K.; Wu, Y.; Wu, W.; Zhang, Q.; Chen, B.; Tian, H.; Zhu, W. Constructing Organic D−A−π−A-Featured Sensitizers with a

Quinoxaline Unit for High-Efficiency Solar Cells: The Effect of an Auxiliary Acceptor on the Absorption and the Energy Level Alignment. *Chem.—Eur. J.* **2012**, *18*, 8190−8200.
(27) Shi, J.; Chen, J.; Chai, Z.; Wang, H.; Tang, R.; Fan, K.; Wu, M.; Han, H.; Qin, J.; Peng, T.; Li, Q.; Li, Z. High Performance Organic Sensitizers Based on 11,12-Bis(hexyloxy)dibenzo[*a*,*c*]phenazine for Dye-Sensitized Solar Cells. *J. Mater. Chem.* **2012**, *22*, 18830−18838.
(28) Li, S.-R.; Lee, C.-P.; Kuo, H.-T.; Ho, K.-C.; Sun, S.-S. High-Performance Dipolar Organic Dyes with an Electron-Deficient Diphenylquinoxaline Moiety in the π-Conjugation Framework for Dye-Sensitized Solar Cells. *Chem.—Eur. J.* **2012**, *18*, 12085−12095.
(29) Pei, K.; Wu, Y.; Islam, A.; Zhang, Q.; Han, L.; Tian, H.; Zhu, W. Constructing High-Efficiency D−A−π−A-Featured Solar Cell Sensitizers: A Promising Building Block of 2,3-Diphenylquinoxaline for Antiaggregation and Photostability. *ACS Appl. Mater. Interfaces* **2013**, *5*, 4986−4995.
(30) Yang, J.; Ganesan, P.; Teuscher, J.; Moehl, T.; Kim, Y. J.; Yi, C.; Comte, P.; Pei, K.; Holcombe, T. W.; Nazeeruddin, M. K.; Hua, J.; Zakeeruddin, S. M.; Tian, H.; Grätzel, M. Influence of the Donor Size in D−π−A Organic Dyes for Dye-Sensitized Solar Cells. *J. Am. Chem. Soc.* **2014**, *136*, 5722−5730.
(31) Lu, X.; Feng, Q.; Lan, T.; Zhou, G.; Wang, Z.-S. Molecular Engineering of Quinoxaline-Based Organic Sensitizers for Highly Efficient and Stable Dye-Sensitized Solar Cells. *Chem. Mater.* **2012**, *24*, 3179−3187.
(32) Lu, X.; Jia, X.; Wang, Z.-S.; Zhou, G. X-Shaped Organic Dyes with a Quinoxaline Bridge for Use in Dye-Sensitized Solar Cells. *J. Mater. Chem. A* **2013**, *1*, 9697−9706.
(33) Ning, Z.; Fu, Y.; Tian, H. Improvement of Dye-Sensitized Solar Cells: What We Know and What We Need to Know. *Energy Environ. Sci.* **2010**, *3*, 1170−1181.
(34) Ning, Z.; Zhang, Q.; Wu, W.; Pei, H.; Liu, B.; Tian, H. Starburst Triarylamine Based Dyes for Efficient Dye-Sensitized Solar Cells. *J. Org. Chem.* **2008**, *73*, 3791−3797.
(35) Chen, C.; Liao, J.-Y.; Chi, Z.; Xu, B.; Zhang, X.; Kuang, D.-B.; Zhang, Y.; Liu, S.; Xu, J. Metal-Free Organic Dyes Derived from Triphenylethylene for Dye-Sensitized Solar Cells: Tuning of the Performance by Phenothiazine and Carbazole. *J. Mater. Chem.* **2012**, *22*, 8994−9005.
(36) Thongkasee, P.; Thangthong, A.; Janthasing, N.; Sudyoadsuk, T.; Namuangruk, S.; Keawin, T.; Jungsuttiwong, S.; Promarak, V. Carbazole-Dendrimer-Based Donor-π-Acceptor Type Organic Dyes for Dye-Sensitized Solar Cells: Effect of the Size of the Carbazole Dendritic Donor. *ACS Appl. Mater. Interfaces* **2014**, *6*, 8212−8222.
(37) Abbotto, A.; Manfredi, N.; Marinzi, C.; Angelis, F. D.; Mosconi, E.; Yum, J.-H.; Zhang, X.; Nazeeruddin, M. K.; Grätzel, M. Di-Branched Di-Anchoring Organic Dyes for Dye-Sensitized Solar Cells. *Energy Environ. Sci.* **2009**, *2*, 1094−1101.
(38) Jiang, X.; Karlsson, K. M.; Gabrielsson, E.; Johansson, E. M. J.; Quintana, M.; Karlsson, M.; Sun, L.; Boschloo, G.; Hagfeldt, A. Highly Efficient Solid-State Dye-Sensitized Solar Cells Based on Triphenylamine Dyes. *Adv. Funct. Mater.* **2011**, *21*, 2944−2952.
(39) Zong, X.; Liang, M.; Fan, C.; Tang, K.; Li, G.; Sun, Z.; Xue, S. Design of Truxene-Based Organic Dyes for High-Efficiency Dye-Sensitized Solar Cells Employing Cobalt Redox Shuttle. *J. Phys. Chem. C* **2012**, *116*, 11241−11250.
(40) Li, Q.; Shi, J.; Li, H.; Li, S.; Zhong, C.; Guo, F.; Peng, M.; Hua, J.; Qina, J.; Li, Z. Novel Pyrrole-Based Dyes for Dye-Sensitized Solar Cells: From Rod-Shape to "H" Type. *J. Mater. Chem.* **2012**, *22*, 6689−6696.
(41) Hong, Y.; Liao, J.-Y.; Cao, D.; Zang, X.; Kuang, D.-B.; Wang, L.; Meier, H.; Su, C.-Y. Organic Dye Bearing Asymmetric Double Donor−π−Acceptor Chains for Dye-Sensitized Solar Cells. *J. Org. Chem.* **2011**, *76*, 8015−8021.
(42) Ren, X.; Jiang, S.; Cha, M.; Zhou, G.; Wang, Z.-S. Thiophene-Bridged Double D−π−A Dye for Efficient Dye-Sensitized Solar Cell. *Chem. Mater.* **2012**, *24*, 3493−3499.
(43) Guo, Z.-H.; Lei, T.; Jin, Z.-X.; Wang, J.-Y.; Pei, J. T-Shaped Donor-Acceptor Molecules for Low-Loss Red-Emission Optical Waveguide. *Org. Lett.* **2013**, *15*, 3530−3533.
(44) Phillips, K. E. S.; Katz, T. J.; Jockusch, S.; Lovinger, A. J.; Turro, N. J. Synthesis and Properties of an Aggregating Heterocyclic Helicene. *J. Am. Chem. Soc.* **2001**, *123*, 11899−11907.
(45) Bijleveld, J. C.; Shahid, M.; Gilot, J.; Wienk, M. M.; Janssen, R. A. J. Copolymers of Cyclopentadithiophene and Electron-Deficient Aromatic Units Designed for Photovoltaic Applications. *Adv. Funct. Mater.* **2009**, *19*, 3262−3270.
(46) Chitoshi, K.; Shoji, T.; Yoshiro, Y. Design of Narrow-Bandgap Polymers Syntheses and Properties of Monomers and Polymers Containing Aromatic-Donor and *o*-Quinoid-Acceptor Units. *Chem. Mater.* **1996**, *8*, 570−578.
(47) Chang, Y. J.; Watanabe, M.; Chou, P.-T.; Chow, T. J. [2.2]Paracyclophane as a Bridging Unit in the Design of Organic Dyes for Sensitized Solar Cells. *Chem. Commun.* **2012**, *48*, 726−728.
(48) Majo, V. J.; Perumal, P. J. One-Pot Synthesis of Heterocyclic β-Chlorovinyl Aldehydes Using Vilsmeier Reagent. *J. Org. Chem.* **1996**, *61*, 6523−6525.
(49) Wade, S.; Suzuki, H. Calcite and Fluorite as Catalyst for the Knövenagel Condensation of Malononitrile and Methyl Cyanoacetate under Solvent-Free Conditions. *Tetrahedron Lett.* **2003**, *44*, 399−401.
(50) Grabowski, Z. R.; Rotkiewicz, K.; Rettig, W. Structural Changes Accompanying Intramolecular Electron Transfer: Focus on Twisted Intramolecular Charge-Transfer States and Structures. *Chem. Rev.* **2003**, *103*, 3899−4032.
(51) Justin Thomas, K. R.; Hsu, Y.-C.; Lin, J. T.; Lee, K.-M.; Ho, K.-C.; Lai, C.-H.; Cheng, Y.-M.; Chou, P.-T. 2,3-Disubstituted Thiophene-Based Organic Dyes for Solar Cells. *Chem. Mater.* **2008**, *20*, 1830−1840.
(52) Zhu, W.; Wu, Y.; Wang, S.; Li, W.; Li, X.; Chen, J.; Wang, Z.-S.; Tian, H. Organic D−A−π−A Solar Cell Sensitizers with Improved Stability and Spectral Response. *Adv. Funct. Mater.* **2011**, *21*, 756−763.
(53) Cai, L.; Tsao, H. N.; Zhang, W.; Wang, L.; Xue, Z.; Grätzel, M.; Liu, B. Organic Sensitizers with Bridged Triphenylamine Donor Units for Efficient Dye-sensitized Solar Cells. *Adv. Energy Mater.* **2012**, *3*, 200−205.
(54) Hagfeldt, A.; Grätzel, M. Light-Induced Redox Reactions in Nanocrystalline Systems. *Chem. Rev.* **1995**, *95*, 49−68.
(55) Wang, Z.-S.; Koumura, N.; Cui, Y.; Takahashi, M.; Sekiguchi, H.; Mori, A.; Kubo, T.; Furube, A.; Hara, K. Hexylthiophene-Functionalized Carbazole Dyes for Efficient Molecular Photovoltaics: Tuning of Solar-Cell Performance by Structural Modification. *Chem. Mater.* **2008**, *20*, 3993−4003.
(56) Hagfeldt, A.; Boschloo, G.; Sun, L.; Kloo, L.; Pettersson, H. Dye-Sensitized Solar Cells. *Chem. Rev.* **2010**, *110*, 6595−6663.
(57) Frisch, M. J.; Trucks, G. W.; Schlegel, H. B.; Scuseria, G. E.; Robb, M. A.; Cheeseman, J. R.; Montgomery, J. A.; Vreven, J. T.; Kudin, K. N.; Burant, J. C.; Millam, J. M.; Iyengar, S. S.; Tomasi, J.; Barone, V.; Mennucci, B.; Cossi, M.; Scalmani, G.; Rega, N.; Petersson, G. A.; Nakatsuji, H.; Hada, M.; Ehara, M.; Toyota, K.; Fukuda, R.; Hasegawa, J.; Ishida, M.; Nakajima, T.; Honda, Y.; Kitao, O.; Nakai, H.; Klene, M.; Li, X.; Knox, J. E.; Hratchian, H. P.; Cross, J. B.; Bakken, V.; Adamo, C.; Jaramillo, J.; Gomperts, R.; Stratmann, R. E.; Yazyev, O.; Austin, A. J.; Cammi, R.; Pomelli, C.; Ochterski, J. W.; Ayala, P. Y.; Morokuma, K.; Voth, G. A.; Salvador, P.; Dannenberg, J. J.; Zakrzewski, V. G.; Dapprich, S.; Daniels, A. D.; Strain, M. C.; Farkas, O.; Malick, D. K.; Rabuck, A. D.; Raghavachari, K.; Foresman, J. B.; Ortiz, J. V.; Cui, Q.; Baboul, A. G.; Clifford, S.; Cioslowski, J.; Stefanov, B. B.; Liu, G.; Liashenko, A.; Piskorz, P.; Komaromi, I.; Martin, R. L.; Fox, D. J.; Keith, T.; Al-Laham, M. A.; Peng, C. Y.; Nanayakkara, A.; Challacombe, M.; Gill, P. M. W.; Johnson, B.; Chen, W.; Wong, M. W.; Gonzalez, C.; Pople, J. A. *Gaussian03*, revision C.02; Gaussian, Inc.: Wallingford, CT, 2004.
(58) Marinado, T.; Nonomura, K.; Nissfolk, J.; Karlsson, M. K.; Hagberg, D. P.; Sun, L.; Mori, S.; Hagfeldt, A. How the Nature of Triphenylamine-Polyene Dyes in Dye-Sensitized Solar Cells Affects

the Open-Circuit Voltage and Electron Lifetimes. *Langmuir* **2009**, *26*, 2592−2598.
(59) Schlichthorl, G.; Huang, S. Y.; Sprague, J.; Frank, A. J. Band Edge Movement and Recombination Kinetics in Dye-Sensitized Nanocrystalline TiO_2 Solar Cells: A Study by Intensity Modulated Photovoltage Spectroscopy. *J. Phys. Chem. B* **1997**, *101*, 8141−8155.
(60) Neale, N. R.; Kopidakis, N.; Lagemaat, J.; Grätzel, M.; Frank, A. J. Effect of a Coadsorbent on the Performance of Dye-Sensitized TiO_2 Solar Cells: Shielding versus Band-Edge Movement. *J. Phys. Chem. B* **2005**, *109*, 23183−23189.
(61) Duffy, N. W.; Peter, L. M.; Rajapakse, R. M. G.; Wijayantha, K. G. U. Investigation of the Kinetics of the Back Reaction of Electrons with Tri-Iodide in Dye-Sensitized Nanocrystalline Photovoltaic Cells. *J. Phys. Chem. B* **2000**, *104*, 8916−8919.
(62) Miyashita, M.; Sunahara, K.; Nishikawa, T.; Uemura, Y.; Koumura, N.; Hara, K.; Mori, A.; Abe, T.; Suzuki, E.; Mori, S. Interfacial Electron-Transfer Kinetics in Metal-Free Organic Dye-Sensitized Solar Cells: Combined Effects of Molecular Structure of Dyes and Electrolytes. *J. Am. Chem. Soc.* **2008**, *130*, 17874−17881.
(63) Wang, Z.-S.; Kawauchi, H.; Kashima, T.; Arakawa, H. Significant Influence of TiO_2 Photoelectrode Morphology on the Energy Conversion Efficiency of N719 Dye-Sensitized Solar Cell. *Coord. Chem. Rev.* **2004**, *248*, 1381−1389.